An Improved Model Predictive Torque Control for PMSM Drives Based on Duty Cycle Optimization

Minkai Wu[1], Xiaodong Sun[1], Jianguo Zhu[2], Gang Lei[3], and Youguang Guo[3]
[1]Automotive Engineering Research Institute, Jiangsu University, Zhenjiang 212013, China
[2] School of Electrical and Information Engineering, University of Sydney, Sydney, NSW2006, Australia
[3]School of Electrical and Data Engineering, University of Technology Sydney, NSW 2007, Australia

This paper proposes an optimal scheme for an interior permanent-magnet synchronous motor (IPMSM) in electric vehicle drive system using novel model predictive torque control (MPTC) algorithm. A single optimal voltage space vector (VSV) is applied with a two-level voltage source inverter in the conventional MPTC. An improved MPTC is presented to reduce the drawbacks with satisfied torque reaction performance without adding the sampling time. Firstly, set switching table to alleviate the calculated complexity which decreasing the selection of the appropriate VSVs. Secondly, optimize the duty cycle to restrain the torque ripple. Finally, the conventional MPTC and the proposed MPTC are compared in the aspects of torque and flux ripples, current harmonics and computational level in the experiment using dSPACE.

***Index Terms*—Interior permanent magnet synchronous motor (IPMSM), model predictive torque control (MPTC), voltage space vector (VSV), torque ripples.**

I. Introduction

Electric vehicles (EVs) have the advantages of pollution and low noise, which is an important way to solve the problems of energy shortage and air pollution in cities [1-3]. In the application of the interior permanent-magnet synchronous motor (IPMSM) drive system of new energy vehicle, the torque is stronger than the surface permanent-magnet synchronous motor (SPMSM) drive [4] and [5]. Therefore, the goal of optimization is generally torque performance by the control algorithm of vehicle IPMSM, including torque response and torque ripples.

There are various kinds of control methods for PMSM drives, such as the field-oriented control (FOC) and direct torque control (DTC) [6]. With the increasing demands of electric drive system and recent advancements in the digital signal processing area, model predictive control (MPC) comes into reality as an efficient control scheme. In addition, finite set model predictive control (FS-MPC) becomes a popular control strategy because of its high performance, fast dynamic response and strong robustness. Meanwhile, it is easy to establish model, no need for accurate model and complex control parameter design. Depending on the different controlled variables in the cost function, FS-MPC is named as model predictive current control (MPCC) and model predictive torque control (MPTC) [7] and [8], respectively. MPCC generates the suitable voltage vector based on the stator current a moment before. MPTC is a control scheme which pays attention to high-performance torque control. However, MPTC is not sensitive about rotor position compared to MPCC. And MPTC produces lower torque ripple with the help of optimal tuning procedure on the weight factor. The conventional MPTC has high torque ripple due to a single pulse control and complex computation [9]. Some literature has proposed duty cycle control for MPTC to improve the control performance. Duty-cycle based MPCT (DCMPTC) uses one active vector and one zero vector in each control cycle. Two duty-cycle control methods are proposed to achieve optimal vector selection and vector duration in the literature [10]. The literature [11] also proposes two voltage vectors, which include an active vector and a null vector, are applied during one control period to improve steady-state performance. In [12], the vector selection and its duration are optimized simultaneously for an improved MPTC with duty cycle control.

In this paper, in order to reduce the computational burden, the switching table consisting of active predictive vectors is set to predict the appropriate voltage space vectors (VSVs). Then, the torque and flux ripples are reduced by optimizing the duty cycle. The proposed predictive control is implemented in dSPACE and applied to an IPMSM. Finally, experimental results are presented to verify the performance of the proposed MPTC.

II. Mathematical Model of IPMSM

The IPMSM is driven by a two-level voltage source inverter and eight switch states are generated in Fig. 1. The continuous time model of IPMSM in the α-β axis stationary reference rotor frame can be written as:

$$\begin{cases} u_\alpha = Ri_\alpha + \dot{\psi}_\alpha \\ u_\beta = Ri_\beta + \dot{\psi}_\beta \end{cases} \tag{1}$$

where $u_{\alpha,\beta}$, $\psi_{\alpha,\beta}$ and $i_{\alpha,\beta}$ are the stationary reference frame components of voltage, flux and current, respectively, R is the stator resistance. In (1), the stator flux in the α-β frame are presented as follow:

$$\begin{cases} \psi_\alpha = L_\alpha i_\alpha + L_{\alpha\beta} i_\beta + \psi_f \cos(\theta_e) \\ \psi_\beta = L_\beta i_\beta + L_{\alpha\beta} i_\alpha + \psi_f \sin(\theta_e) \end{cases} \tag{2}$$

where $L_{\alpha\beta}$ is the mutual inductance, $L_{\alpha,\beta}$ are the stationary reference frame components of stator inductances, ψ_f is the permanent magnet flux, and θ_e is the electrical rotor position. Combined with (1) and (2), the voltage equations of the IPMSM are given as:

$$\begin{cases} u_\alpha = Ri_\alpha + L_\alpha \dfrac{di_\alpha}{dt} + L_{\alpha\beta} \dfrac{di_\beta}{dt} - \omega_e \psi_f \sin\theta_e \\ u_\beta = Ri_\beta + L_\beta \dfrac{di_\beta}{dt} + L_{\alpha\beta} \dfrac{di_\alpha}{dt} + \omega_e \psi_f \cos\theta_e \end{cases} \tag{3}$$

where L_α=L_0+L_1cos2θ_e, L_β=L_0-L_1cos2θ_e, $L_{\alpha\beta}$=L_1sin2θ_e, L_0=$\frac{L_d+L_q}{2}$, L_1=$\frac{L_d-L_q}{2}$, L_d, L_q are dq-axis inductances and ω_e is rotor electrical angular velocity. Finally, the electromagnetic torque is shown as:

$$T_e = \frac{3}{2} p(\psi_\alpha i_\beta - \psi_\beta i_\alpha) \tag{4}$$

where T_e is the electromagnetic torque, and p is the number of pole pairs. MPTC is implemented with a discrete time model based on the Euler forward differentiation method for the instant time (k+1) as follows:

$$\begin{cases} i_\alpha(k+1) = i_\alpha(k) + \dfrac{T_s}{L_\beta L_\alpha - L_{\alpha\beta}^2}[(L_\beta u_\alpha - L_{\alpha\beta} u_\beta) \\ -R(L_\beta i_\alpha - L_{\alpha\beta} i_\beta) + \omega_e \psi_f (L_{\alpha\beta} \cos\theta_e + L_\beta \sin\theta_e)] \\ i_\beta(k+1) = i_\beta(k) + \dfrac{T_s}{L_\alpha L_\beta - L_{\alpha\beta}^2}[(L_\alpha u_\beta - L_{\alpha\beta} u_\alpha) \\ -R(L_\alpha i_\beta - L_{\alpha\beta} i_\alpha) + \omega_e \psi_f (L_\alpha \cos\theta_e + L_{\alpha\beta} \sin\theta_e)] \end{cases} \tag{5}$$

$$\theta_e(k+1) = \theta_e(k) + T_s \omega_e \tag{6}$$

where T_s is the sampling time.

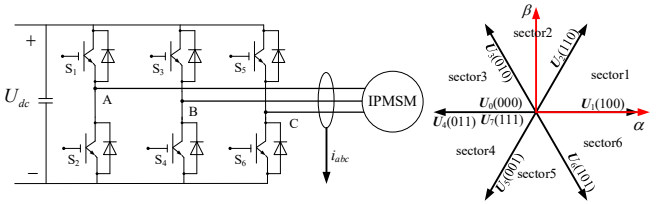

(a) (b)

Fig. 1. Two-level voltage source inverter. (a) Topology of three-phase full bridge inverter, (b) Voltage space vectors of different switch states

III. Proposed Model Predictive Torque Control

The block diagram of the proposed MPTC is demonstrated in Fig. 2. The proposed MPTC is improved by adding active predictive vectors option table. In addition, the duty cycle optimization is presented with the calculation of torque. The flux weakening is not taken into account. Therefore, the flux amplitude remains constant.

The speed loop is controlled by proportional integral (PI) controller. Proportional adjustment immediately reduces the deviation when the deviation produces. Proportional coefficient can quicken the response and reduce the error. However, too large coefficient will decline the stability of the system. Integral controller eliminates the steady-state error and improves the error free degree.

A. Vector Selection

In this paper, the design of cost function is based on the principle of the minimum torque ripple, and the torque and flux are used as the evaluation indexes of the controller performance. The controlled variables are predicted for instant time (k+1) from discrete model.

$$F = \left|T_e^*\right| - \left|T_e(k+1)\right| + Q\left|\psi_s^*\right| - \left|\psi_s(k+1)\right| \tag{7}$$

where T_e^* and ψ_s^* are the reference of torque and flux linkage, respectively. The coefficient Q is the adjustment coefficient due to the different dimensions of torque and flux and F is the cost function. Q plays an important role in the performance motor drive system using MPTC. Some guidelines are referred to ensure the suitable value of Q in [13]. In the conventional MPTC, all possible VSVs are substituted into (7) to achieve the optimal VSV. However, it will increase the computational burden. In order to reduce the amount of calculation, a active predictive vectors option table is given.

When considering the dynamic of torque, it is necessary to select four possible VSVs with clockwise and anticlockwise direction of rotation. As for the stator flux performance, it is already contained during the minimum of the cost function. Active predictive vectors are selected by the position of the stator flux θ_f and torque offset ΔT_e given in (8) and (9).

$$\theta_f = \arctan(\frac{\psi_\beta}{\psi_\alpha}) \tag{8}$$

$$\Delta T_e = T_e^* - T_e \tag{9}$$

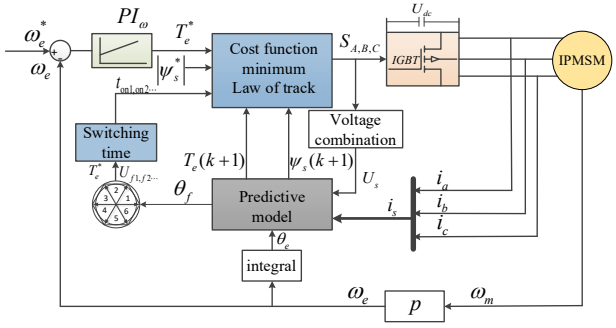

Fig. 2. Block diagram of the proposed MPTC.

The principle of selecting two possible active VSVs (AVSV) is depended on the position of the stator flux θ_f and torque offset ΔT_e, which is shown in Table I. The case of zero torque offset is not supplied in Table I because one zero VSV (ZVSV) U_0 aims at this case. In order to reduce the switch loss, only one bridge arm is changed to produce fewer switching transitions with the application of U_0 and U_7.

TABLE I
Possible Active VSVs

ΔT_e	θ_f					
	S1	S2	S3	S4	S5	S6
>0	U_2, U_3	U_3, U_4	U_4, U_5	U_5, U_6	U_6, U_1	U_1, U_2
<0	U_5, U_6	U_6, U_1	U_1, U_2	U_2, U_3	U_3, U_4	U_4, U_5

B. Duty Cycle Optimization

Different from the conventional MPTC applying the VSV during the whole control cycle, the proposed MPTC applies one AVSV and one ZVSV during each control cycle. Because of the torque inertial delay impact, mean torque control has an advantage to predict the value of the torque of the PMSM. Therefore, the duty cycle of AVSV is obtained by the principle

of the mean torque control. The principle of the mean torque control is shown in Fig. 3. It can be assumed that the torque performance is linearized to predict the magnitude of the torque at (k+1). One AVSV is applied to the inverter for a t_{on} time and one ZVSV is applied for the rest of the control duty cycle t_{off}. The torque at (k+1) can be predict as:

$$T_e(k+1) = T_e(k) + l_1 t_{on} + l_2 t_{off} = T_e^* - \frac{1}{2}\delta T \tag{10}$$

where l_1 and l_2 are the differential coefficients of torque for AVSV and ZVSV, respectively. The mean torque control has a function to keep the torque within the bandwidth of torque inertial delay δT, which can be calculated as:

$$\delta T = -\frac{l_1 l_2}{l_1 - l_2} T_s \tag{11}$$

By solving (10) and using (11) for the switching time t_{on}, it can be calculated through the AVSVs, the currents, the stator flux position and the electrical rotor position. Thus, the switching time t_{on} for the application of AVSV is obtained as:

$$t_{on} = \frac{T_e^* - \frac{\delta T}{2} - T_e(k) - l_2 T_s}{l_1 - l_2} \tag{12}$$

And the rest of the control duty cycle t_{off} for ZVSV can be calculated as:

$$t_{off} = T_s - t_{on} \tag{13}$$

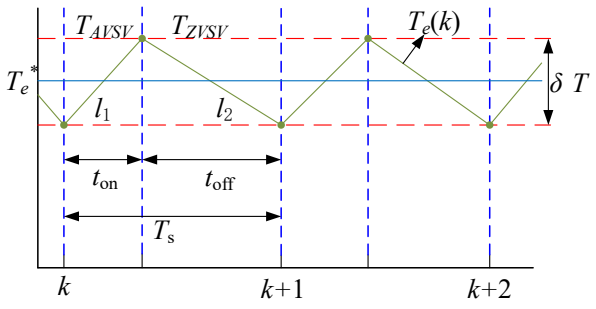

Fig. 3. Principle of the mean torque control

C. The Proposed MPTC

The conventional MPTC has two methods for the vector selection and duty cycle optimization. The one is that the process of vector selection and duty cycle optimization are implemented separately. This method only ensures optimal VSV applied for the whole control cycle. The other is that the vector selection and duty cycle optimization are performed simultaneously. However, this control method ensures the AVSV and ZVSV that minimize the cost function. Therefore, this control method needs much computational time.

In the proposed MPTC, the process of vector selection and duty cycle optimization are implemented before evaluating the cost function. Rather to evaluate all possible VSVs, the proposed MPTC only selects three possible VSVs in Table I. Soon after, the computational time is reduced and the torque performance is not affected due to the mean torque control. The respective switching time t_{on} for three possible VSVs are calculated by (12) and the variables in (k+1) are predicted. However, the voltage is only applied during the t_{on} instead of the whole control cycle. In this way, the current prediction is given again:

$$\begin{cases} i_\alpha(k+1) = i_\alpha(k) + \dfrac{L_\beta u_\alpha - L_{\alpha\beta} u_\beta}{L_\beta L_\alpha - L_{\alpha\beta}^2} t_{on} + \dfrac{T_s}{L_\beta L_\alpha - L_{\alpha\beta}^2} \\ [-R(L_\beta i_\alpha - L_{\alpha\beta} i_\beta) + \omega_e \psi_f (L_{\alpha\beta}\cos\theta_e + L_\beta \sin\theta_e)] \\ i_\beta(k+1) = i_\beta(k) + \dfrac{L_\alpha u_\beta - L_{\alpha\beta} u_\alpha}{L_\alpha L_\beta - L_{\alpha\beta}^2} t_{on} + \dfrac{T_s}{L_\alpha L_\beta - L_{\alpha\beta}^2} \\ [-R(L_\alpha i_\beta - L_{\alpha\beta} i_\alpha) + \omega_e \psi_f (L_\alpha \cos\theta_e + L_{\alpha\beta} \sin\theta_e)] \end{cases} \tag{14}$$

Applying the same principle, flux prediction can be obtained as:

$$\psi_{\alpha\beta}(k+1) = \psi_{\alpha\beta}(k) + u_{\alpha\beta} t_{on} - R\int_{kT_s}^{(k+1)T_s} i_{\alpha\beta}(k)dt \tag{15}$$

As can be seen there is a digital integration in the equation of flux prediction. Therefore, it produces a voltage offset at the whole control cycle. In order to solve this problem, a linear approximation is applied. The current has a law of track during the application of the AVSV and the ZVSV without considering the small sampling time. The equation of current highly depends on machine parameters. Nevertheless, mean current value can simply the (15) to obtain the final flux prediction.

$$\begin{cases} \psi_\alpha(k+1) = \psi_\alpha(k) + (L_\beta u_\alpha - L_{\alpha\beta} u_\beta) t_{on} - RT_s \\ [(L_\beta i_\alpha - L_{\alpha\beta} i_\beta) + \dfrac{L_\beta u_\alpha - L_{\alpha\beta} u_\beta}{2(L_\beta L_\alpha - L_{\alpha\beta}^2)}] \\ \psi_\beta(k+1) = \psi_\beta(k) + (L_\alpha u_\beta - L_{\alpha\beta} u_\alpha) t_{on} - RT_s \\ [(L_\alpha i_\beta - L_{\alpha\beta} i_\alpha) + \dfrac{L_\alpha u_\beta - L_{\alpha\beta} u_\alpha}{2(L_\alpha L_\beta - L_{\alpha\beta}^2)}] \end{cases} \tag{16}$$

According to the application of the proposed MPTC, one AVSV and one ZVSV during each sampling time are operated. However, the proposed control scheme guarantees the switching time t_{on} to the maximum value (smaller than sampling time). Thus, the switching time keeps a constant, which reduces the cost of switch.

IV. Experimental Results

In order to evaluate the performance of the proposed MPTC, both the conventional MPTC and the proposed MPTC are tested in a dSPACE DS1007 PPC. The experimental setup is shown in Fig. 4. The sampling frequency of each control method is set 10 kHz to limit the switching frequency below the maximum value (20 kHz) of IGBT. In the real-time interface (RTI) of dSPACE, the switching frequencies are all set as 10 kHz. The delay of the digital signal processors is generated because the controller output cannot be applied immediately. To overcome this problem, the delay compensation mentioned in [10] is used. The main parameters of the IPMSM are listed in Table II.

TABLE II
IPMSM Drive System Parameters

Parameter	Symbol	Value
Number of pole pairs	P	5

Stator resistance	R_s	0.18 Ω
d-axis inductance	L_d	0.174 mH
q-axis inductance	L_q	0.29 mH
Permanent-magnet flux linkage	ψ_f	0.0711 Wb
Inertia	J	0.067 kgm^2
Rated speed	N	2000 rpm
Rated power	P_N	60 kW

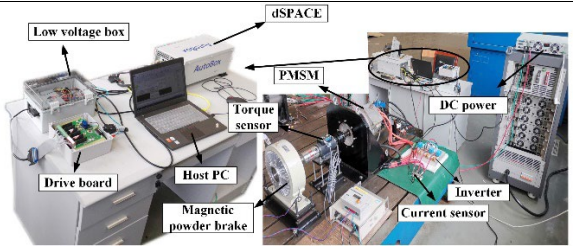

Fig. 4. Experimental setup

A. Dynamic Torque Response with Speed Change

For the experiment, two situations are considered for the starting process, no-load and load, then speed/load changes are applied to the drive system to investigate the dynamic responses. The proposed MPTC are compared with the conventional MPTC in the aspect of torque and stator flux ripples to indicate the superiority, respectively. Fig. 5 shows the dynamic torque response with speed change. For each control method, four response curves are given. They are the rotor speed Nr (rpm), flux ripple ψ_s (Wb), electromagnetic torque T_e (Nm) and stator phase-a current I_a (A) from the top to bottom. The initial reference speed for the starting process is 1200 rpm, then a speed change (from 1200 to rated speed 2000 rpm) is applied at time 0.15 s and a load torque change (from 0 to 10 Nm) is applied at 0.35 s. As shown, the conventional MPTC has a relatively large overshoot when the rotor speed reaches 1200 rpm and changes to 2000 rpm at 0.15 s. The torque and flux ripples are reduced 2.64 Nm and 0.025 Wb, respectively. The system has a low frequency oscillation, which is judged by whether the interval of the negative current component of the inverter input is more than $1/f_c$ (f_c is the carrier wave frequency of the inverter) or not. In Fig.8, the switching frequency of the conventional MPTC and the proposed MPTC are different. In the propose MPTC, f_c is close to the switching frequency and the system is underdamped. Therefore, there are a low frequency oscillation in the proposed MPTC method. In the later research, it can be avoidable to change f_c.

B. Dynamic Torque Response with Stable Speed

Fig. 6 shows the dynamic responses of two control methods for the IPMSM drive system with an initial load torque reference of 15 Nm and an initial reference speed of 2000 rpm. The following four waveforms are illustrated, which are the rotor speed Nr (rpm), flux ripple ψ_s (Wb), electromagnetic torque T_e (Nm) and stator phase-a current I_a (A). The load torque changes twice, from 15 to 0 Nm at 0.15 s and from 0 to 10 Nm at 0.35 s. It can be observed that the proposed MPTC has smaller speed overshoot. Furthermore, the torque and flux ripples are reduced 1.74 Nm and 0.012 Wb, respectively.

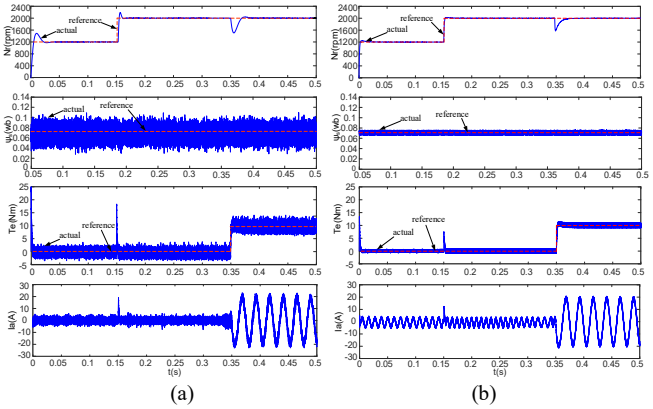

(a) (b)

Fig. 5. Experiment of torque response with speed change. (a) Conventional MPTC. (b) Proposed MPTC.

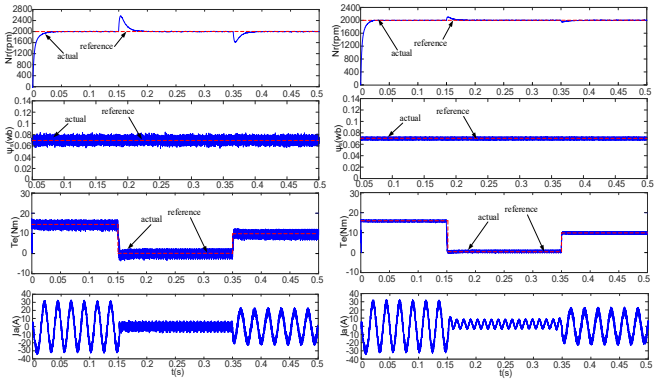

(a) (b)

Fig. 6. Experiment of torque response with stable speed. (a) Conventional MPTC. (b) Proposed MPTC.

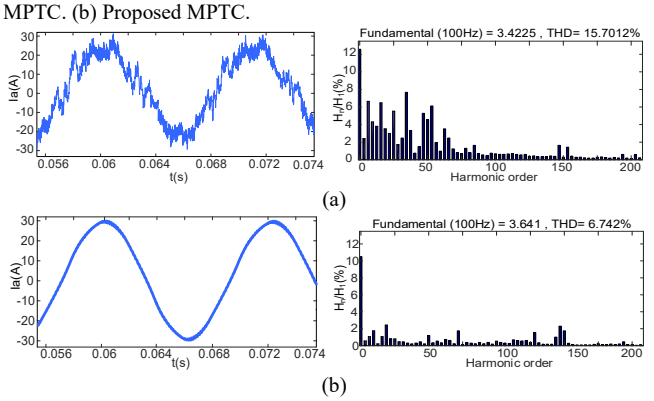

(a)

(b)

Fig. 7. Harmonic spectrum of stator current at 2000 rpm with load torque. (a) Conventional MPTC. (b) Proposed MPTC.

C. Current Total Harmonic Distortion (THD) Analyze and Switching Frequency

The current THD analyze is shown in Fig. 7 for two control schemes. The harmonics are calculated to 20kHz (200th-order harmonics). It is clear that the low order harmonics in the proposed MPTC are much lower than the conventional MPTC. The current THD of the conventional MPTC is 15.7%. It is higher than the value of the proposed MPTC. Therefore, the proposed MPTC has better performance in the reduction of current harmonics. Moreover, the computational time of dSPACE for the conventional MPTC and the proposed MPTC are 25.4 and 18.1 μs. The proposed MPTC has less computational time, which illustrates the reductive calculated complexity.

One AVSV and one ZVSV during each sampling time are operated in the proposed MPTC. It causes a higher switching frequency than the conventional MPTC. Fig. 8 shows the evaluation of the switching frequency of two control methods at different speeds and loads. As can be seen that switching frequency of the proposed MPTC is higher than that of the conventional MPTC. The average value of the switching frequency is 5.3 kHz and 6.4 kHz, respectively. Due to the duty circle optimization, the switching frequency increases. On the contrary, the conventional MPTC may apply the same VSV in the following control cycle. The above explanation is account for the increase of the switching frequency and a stable switching frequency for the proposed MPTC. However, the conventional MPTC has variable frequency. Although the switching frequency of the proposed MPTC is higher than that of the conventional MPTC. The higher switching frequency is lower than the limit of maximum value (20 kHz) of IGBT and the difference value is about 1 kHz. Meanwhile, the proposed MPTC presents more effective control performance.

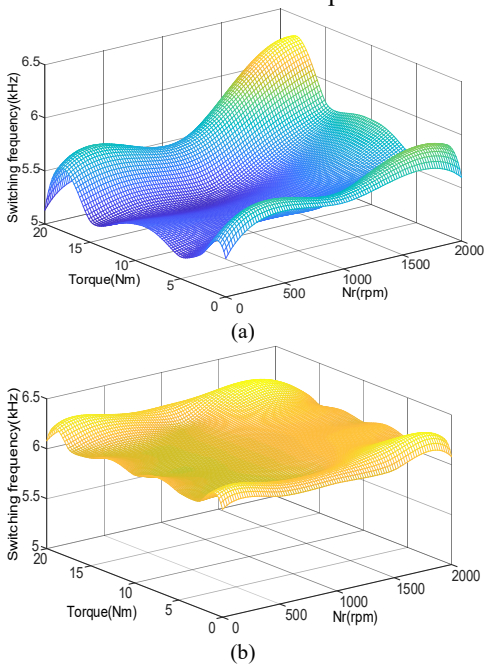

Fig. 8. Switching frequency. (a) Conventional MPTC. (b) Proposed MPTC.

V. Conclusion

EVs have high requirement for torque. Therefore, the conventional MPTC is not suitable for the application of EVs. A single VSV is used during the control circle, which causes the high torque ripple. This paper proposes an improved MPTC to reduce the torque and flux ripples, as well as current THD. In this study, the duty cycle optimization is based on the mean torque control principle to obtain the switching time t_{on} and t_{off}. Then, the torque and flux ripples are reduced by the duty cycle optimization. In order to reduce the computational time, the switching table consisting of active predictive vectors is set to predict the appropriate VSVs. The experimental results present that the proposed MPTC has an advantage over reducing the torque and flux ripples for dynamic torque response. In addition, the current THD is also reduced for a better motor drive performance.

Acknowledgment

This work was supported by the National Natural Science Foundation of China under Project 51875261, the Natural Science Foundation of Jiangsu Province of China under Projects BK20180046, and BK20170071, and the “Qinglan project” of Jiangsu Province.

References

[1] Z. Xiang, *et. al,* “Multilevel design optimization and operation of a brushless double mechanical port flux-switching permanent-magnet motor,” *IEEE Trans. Ind. Electron.*, vol. 63, no. 10, pp. 6042-6054, Oct. 2016.

[2] X. Sun, C. Hu, G. Lei, Z. Yang, Y. Guo, and J. Zhu, “Speed sensorless control of SPMSM drives for EVs with a binary search algorithm-based phase-locked loop,” *IEEE Trans. Veh. Technol.*, vol. 69, no. 5, pp. 4968-4978, May 2020.

[3] X. Zhu, J. Huang, L. Quan, Z. Xiang, and B. Shi, “Comprehensive sensitivity analysis and multi-objective optimization research of permanent magnet flux-intensifying motors,” *IEEE Trans. Ind. Electron.*, vol. 66, no. 4, pp. 2613-2627, Apr. 2019.

[4] Z. Shi, *et. al,* “Torque analysis and dynamic performance improvement of a PMSM for EVs by skew angle optimization,” *IEEE Trans. Appl. Supercon.*, vol. 29, no. 2, Art. no. 0600305, Mar. 2019.

[5] X. Sun, M. Wu, G. Lei, Y. Guo, and J. Zhu, “An improved model predictive current control for PMSM drives based on current track circle,” *IEEE Trans. Ind. Electron.*, 2020, DOI: 10.1109/TIE.2020.2984433.

[6] X. Sun, C. Hu, Gang Lei, Y. Guo, and J. Zhu, “State feedback control for a PM hub motor based on grey wolf optimization algorithm,” *IEEE Trans. Power Electron.*, vol. 35, no. 1, pp. 1136-1146, Jan. 2020.

[7] W. Xie, X. Wang, F. Wang, W. Xu, R. Kennel, and D. Gerling, “Dynamic loss minimization of finite control set-model predictive torque control for electric drive system,” *IEEE Trans. Power Electron*., vol. 31, no. 1, pp. 849–860, Jan. 2016.

[8] X. Sun, *et al*., “MPTC for PMSMs of EVs with multi-motor driven system considering optimal energy allocation,” *IEEE Trans. Magn.*, vol. 55, no. 7, Art. no. 8104306, Jul. 2019.

[9] A. Mora, Á. Orellana, J. Juliet, and R. Cárdenas, “Model predictive torque control for torque ripple compensation in variable-speed PMSMs,” *IEEE Trans. Ind. Electron.*, vol.63, no. 7, pp. 4584-4592, Mar. 2016.

[10] Y. Zhang, D. Xu, J. Liu, S. Gao, and W. Xu, “Performance improvement of model-predictive current control of permanent magnet synchronous motor drives,” *IEEE Trans. Ind. Appl.,* vol. 53, no. 4, pp. 3683-3695, Jul./Aug. 2017.

[11] X. Zhang, and B. Hou, “Double vectors model predictive torque control without weighting factor based on voltage tracking error,” *IEEE Trans. Power. Electron*., vol. 33, no. 3, pp. 2368–2380, Mar. 2018.

[12] Y. Zhang, and H. Yang, “Model predictive torque control of induction motor drives with optimal duty cycle control,” *IEEE Trans. Power. Electron*., vol. 29, no. 12, pp. 6593–6603, Dec. 2014.

[13] Cortes. P, Kouro. S, La Rocca. B, *et al*., “Guidelines for weighting factors design in model predictive control of power converters and drives,” *IEEE Int. Conf. on Industrial Technology, Gippsland, Australia*., pp. 1–7, Feb. 2009.